

Numerical Simulation of Supersonic Combustion with Parallel Injection of Hydrogen Fuel

M.S.R. Chandra Murty*, R.D. Mishal# and Debasis Chakraborty*

*Defence Research and Development Laboratory, Hyderabad-500 058

#Defence Institute of Advanced Technology, Pune-411 025

E-mail: debasis_cfd@drdl.drdo.in

ABSTRACT

Thermochemical exploration of mixing and combustion of parallel hydrogen injection into supersonic vitiated air stream in a divergent duct is presented. Three-dimensional Navier Stokes equations along with two-equation turbulence models and Eddy dissipation concept (EDC)-based combustion models are solved using commercial CFD software. Chemical reaction for H_2 -air system is modelled by two different simple chemical kinetic schemes namely; infinitely fast rate kinetics as well as the single-step finite rate kinetics. Grid convergence of the solution is demonstrated and a grid convergence index-based error estimate has been provided. Insight into the mixing and combustion of high-speed turbulent reacting flow is obtained through the analysis of various thermochemical variables. Very good comparisons are obtained for the exit profiles for various fluid dynamical and chemical variables for the mixing case. For reacting case, the comparison between the experimental and the numerical values are reasonable. Parametric studies were carried out to study the effect of different turbulence models and turbulent Schmidt numbers. It is seen that Wilcox $k-\omega$ turbulence model performed better than the other two-equation turbulence models in its class. Strong dependence of flow behaviour on turbulent Schmidt number was observed. The results indicate that simple chemical kinetics is adequate to describe the H_2 -air reaction in the scramjet combustor.

Keywords: Numerical simulation, supersonic combustion, hydrogen fuel, turbulent Schmidt number, scramjet combustor

NOMENCLATURE

Latin letters

A, B	Constants in EDM model
F	Factor of safety
h	Grid spacing order
k	Turbulent kinetic energy
p	Order of numerical scheme
R	Mixing rate
r	Stoichiometric ratio
w	Reaction rate
Y	Mass fraction

Greek Symbols

ρ	Density
ε	Turbulent dissipation rate
χ	Fine structure fraction
τ	Time scale
γ	Length fraction of fine scales

Subscripts

ebu,edm	ref. to eddy dissipation model
f	Fuel
o	Oxidiser
p	Product
i	Species index

Superscripts

o	Surrounding fluid
$*$	Fine structure

1. INTRODUCTION

Sustained flight at hypersonic speed in the atmosphere remains the largest unexplored region of the possible flight envelope. Development of air-breathing hypersonic technology has been the subject of renewed interest since the 1980's because of tremendous military and commercial opportunities. The success of efficient design of such a trans-atmospheric hypersonic vehicle depends largely on the proper choice of propulsion system, which is capable of producing large thrust to overcome the drag experienced by the vehicle. This type of vehicle, according to current proposals, uses supersonic combustion ramjet (scramjet) propulsion system.

The development of efficient scramjet engine requires a detailed understanding of the complex mixing and combustion process inside the combustor. The diffusive mode of combustion, in which energy is added gradually, is preferred over the premixed mode in the scramjet combustor to minimise the intake-combustor interaction. The flow field inside the combustor is complex where fluid dynamics and chemistry interact strongly.

Starting from pioneering work of Ferri¹, enormous amount of flow investigations have been performed in various countries on different aspects of scramjet flow field including ignition, flame holding, fuel injection, intake combustor interaction etc. Both hydrogen and kerosene fuels have been considered. In a recent review, Curran² has identified two emerging scramjet applications namely: (i) hydrogen-fuelled engine to access space, and (ii) hydrocarbon-fuelled engines for air-launched missiles. Considerable efforts have been focused on different injection schemes like cavity, strut, and pylon for different geometrical configurations and flow conditions in the past two decades. Selected methods, that have been used to enhance the mixing process in the Scramjet engines, are summarised and reported by Seiner³, *et al.*

With the advent of powerful computers, robust numerical algorithm, CFD is complementing 'difficult to perform' experiment and playing a very major role in the development of scramjet combustor through analysis of various thermochemical parameters obtained from the numerical simulation. Supersonic combustion with hydrogen fuel has been studied extensively both experimentally⁴⁻⁷ and numerically⁸⁻¹³ in the literature. Despite many years of research, large number of issues related to description of combustion in supersonic turbulent reactive flows remains unanswered.

Reduction of losses and increase in momentum are very important for efficient design of scramjet combustor. Parallel injection of hydrogen fuel has often been contemplated in high speed operating envelope of scramjet combustor to reduce the injection losses and to take advantage of incremental momentum of the fuel stream. To generate experimental data on diffusive mixing and reaction of fuel and air at high temperature typical for flight Mach numbers above 6, Burrows and Kurkov⁴ have conducted mixing and combustion experiments where sonic hydrogen was injected in a direction parallel to the main supersonic stream. The parallel stepped-wall injection of hydrogen into the combustor produces minimum disturbance to the free stream flow when the fuel and air pressure are matched. Hydrogen-nitrogen gas mixture is burned with liquid oxygen in the heater at high pressure to produce high temperature gas for the combustor. Mass flow rate of each gas is so regulated that one gets the desired total temperature of the vitiated air stream with 21 per cent (by volume) of oxygen content. For the non-reacting mixing experiments, the vitiated air does not contain any oxygen. In this approach, it is possible to study mixing process independent of combustion under approximately the same conditions as that for the combustion tests. Detailed measurements of exit profiles of various thermo-chemical parameters and the axial distribution of surface pressure provide a good database for validating CFD codes in a clean confined duct.

Kim¹³ simulated the mixing of vitiated air stream and hydrogen with and without chemical reaction pertaining to Burrows and Kurkov experimental conditions and reported

good match between the experimental and the numerical results. Although, turbulence field was described by a multiple time-scale turbulence model¹⁴ and 9 species-24 reaction kinetic mechanism were used to represent H_2 -Air chemical kinetics, no modelling of turbulence-chemistry interaction was presented. Recently, Keistler¹⁵ adopted closure equations^{16,17} for turbulent Schmidt number and turbulent Prandtl number along with k- ϵ turbulence model¹⁸ to study the same experiment. Effect of two H_2 -Air chemical kinetic schemes namely 7 species-7 reaction scheme due to Jachimowski,¹⁹ *et al.* and 9 species-18 reaction scheme due to Connaire,²⁰ *et al.* and the effect of turbulence-chemistry interaction model were investigated. It has been observed that with the addition of turbulence-chemistry interaction, there is a dramatic increase in the turbulent diffusivity throughout the flame region and different chemical schemes do not alter the mixing and combustion process significantly. It is clear that modelling issues in high-speed turbulent reactive flows need further investigation since these turbulence and chemical reaction models are computationally prohibitive for practical engineering calculations.

In this study, mixing and combustion experiments of Burrows and Kurkov⁴ have been explored numerically with standard turbulence model, simple chemical kinetic scheme, and simple turbulence-chemistry interaction model to find the capability of these standard engineering tools to predict overall features of the mixing and reaction of high-speed turbulent reacting flow in a confined duct. Insight into the flow-development process is obtained for parallel injection of hydrogen fuel into supersonic stream. The experimentally measured surface pressure and exit profiles of various fluid dynamical and chemical variables are compared with numerical values.

2. TEST SET UP OF THE COMBUSTOR

The schematic of the test combustor of Burrow & Kurkov experiments is presented in Fig. 1. The first section is a constant area of dimension 51 mm \times 89 mm from facility nozzle exit to combustor entry. The 2-D facility

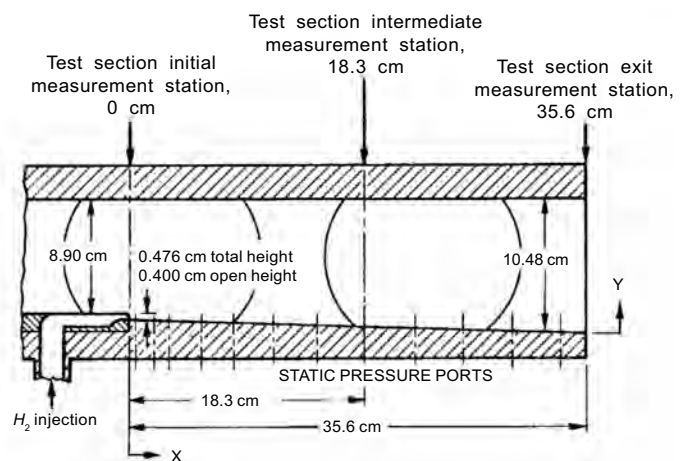


Figure 1. Schematic of Burrows & Kurkov⁴ test combustor.

nozzle provides Mach 2.44 stream with static temperature and static pressure of 1270 K and 1 atmosphere respectively. Gas generator flows were reproducible within ± 1 per cent. At the end of constant area section, sonic hydrogen was injected in the combustor through an injector of 0.76 mm thickness at the top of 4 mm step. After the step, the lower wall was given a divergence angle of 1.78° . So the test section was expanded linearly for 51 mm \times 93.8 mm from the entry to 51 mm \times 104.8 mm at the exit. The length of the combustor from the step to the exit was 356 mm. Hydrogen fuel was heated in a storage heater and total temperature of hydrogen flowing through the slot could be varied from 300 K to 800 K. The properties of the vitiated air and hydrogen stream used for the mixing and combustion cases are summarised in Table 1.

Table 1. Properties of the vitiated air and hydrogen

Parameters	Vitiated air		Hydrogen
	Mixing case	Reacting case	
Mach No.	2.44	2.44	1.0
Total temp (K)	2276	2380	303
Total pressure (bar)	18.5	17.1	1.85
<i>Mole fraction composition:</i>			
X_{H_2}	0.0	0	1.0
X_{H_2O}	0.322	0.373	0.0
X_{O_2}	0.0	0.199	0.0
X_{N_2}	0.678	0.428	0.0

The total pressure and total temperature profiles at the exit section were measured by a specially designed water-cooled pitot pressure probe and thermocouple probe. Water-cooled probes were designed to obtain gas samples and trapped samples were analysed on a mass spectrometer. Instrumentation probes used in the test section were moved incrementally between succeeding runs to obtain the profiles of the parameters in the exit section. Most of the exit profile measurements were made within 40 mm distance from the lower wall. It was observed that the temperature indicated by thermocouple probes were reproducible by ± 3 per cent whereas the pressure measurements were generally within ± 2 per cent except in the reaction zone, where measurement varied over a wide range from run to run. Gas sampling analysis was accurate within ± 2 per cent. The sampling probes were also used as cooled gas pyrometers to indirectly measure the stream total temperature. Static pressure was measured at the entrance of the test section, along the wall downstream from the hydrogen injection step. Four 151 mm diameter quartz windows were mounted flush with the inner wall surface for visual and photographic observations within the test section. Ignition delays were determined from the photographs of *OH* radiation, which originated at various distances downstream from hydrogen injection.

3. COMPUTATIONAL METHODOLOGY

Simulations are carried out using a commercial CFD software Fluent²¹. It solves 3-D Navier stokes equation in a structured, multi-block grid system using a collocated variable arrangement. To simulate high Mach number compressible flow (as in the present case), density-based solver was used along with Roe flux difference splitting scheme²². Spatial discretisation was achieved by second-order upwind scheme and first-order implicit Euler scheme was used for temporal discretisation. Various two-equation turbulence models namely, *k*- ϵ , *k*- ω , Menter's SST *k*- ω , models were used to determine their predictive capability in turbulent reacting flows.

The chemistry of H_2 -air combustion reaction is represented on a molar basis by $H_2 + 0.5O_2 = H_2O$. The mixing rate determined from the Eddy dissipation model (EDM) is given as.

$$R_{k,edm} = -A_{ebu}\rho \frac{\epsilon}{k} \min \left\{ Y_f, \frac{Y_o}{r_k}, B_{ebu} \frac{Y_p}{1+r_k} \right\} \quad (1)$$

where ρ , Y_f , Y_o and Y_p are the density and mass fractions of fuel, oxidiser, and products, respectively, A_{ebu} and B_{ebu} are the model constants, and r_k is the stoichiometric ratio.

In the single-step finite rate chemistry, the following reversible reaction involving H_2 , O_2 and H_2O is considered.



With pre-exponential factor (A) of 1.02×10^{19} , power constant (N) of 0 and activation temperature (E/R) of 8052.

Following Gran²³, the mean reaction rate for the species i (w_i) is given by

$$\frac{\bar{w}_i}{\rho} = \frac{Y_i^2 \chi}{\tau^*} (Y_i^0 - Y_i^*) \quad (3)$$

Where χ is the fraction of the fine structures where reaction occurs and superscripts '0' and '*' refers to the surrounding fluids and fine structure region. τ^* is the time scale for the mass transfer between the fine structures and the surroundings. The fine structure is considered as a constant pressure homogeneous reactor where all the properties are time-dependent and no spatial gradient exists. A more detailed description of the Eddy dissipation concept (EDC)-based finite rate combustion model is also available²¹.

Chakraborty,²⁴ *et al.* has carried out direct numerical simulation (DNS) of H_2 -air mixing layer of Erdos experimental case⁶ and investigated the effect of fast chemistry, single-step chemistry and 7 species-7 reaction finite rate chemistry in the thermo-chemical behaviour of reacting mixing layer. The computed DNS database was used to evaluate the existing combustion models²⁵. It was shown that finite rate EDC-based combustion model could predict the overall trend of reaction rate profiles although the model predicts a thin reaction zone compared to DNS data.

Finite rate calculations were performed using Chemkin[®] software²⁶. A coupling code was written to make calls

between Chemkin and Fluent. At every time step δt , the current solution field were taken from Fluent solver including mass fraction of every species, temperature and pressure. These values were used as initial conditions for Chemkin solver. Chemkin solves the reaction rates for each species and estimates the mass fractions of all species and temperature. These values were transferred to Fluent solver. This process continues for every iteration of Fluent solver.

4. RESULTS AND DISCUSSION

Similar to the experimental conditions, two different cases, namely, mixing case and combustion case, have been simulated. For mixing case, vitiated air stream contained N_2 and H_2O while $H_2 - O_2 - H_2O - N_2$ system was considered for the combustion case.

4.1 Computational Grid and Boundary Condition

A two-dimensional structured grid was generated in the computational domain. 300 grid points were taken in the axial direction and 130 grid points were taken along the vertical direction. Typical grid distribution in the domain is shown in Fig. 2. Grid was stretched exponentially from the inflow plane to exit plane. In the present case, most

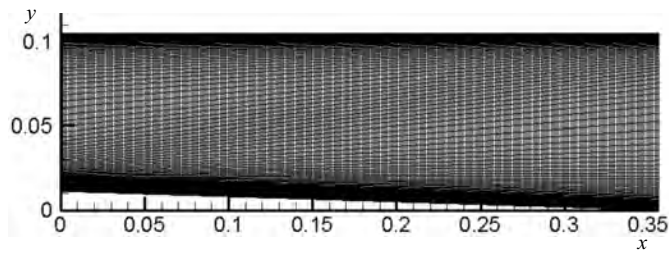


Figure 2. Grid distribution in the computational domain.

of the measurements were made in the vicinity of boundary layer region. Therefore, the boundary layer region was resolved by integrating conservation equations right up to the wall without using wall functions. The minimum grid spacing near the inflow plane was 0.001 mm. To maintain proper wall y^+ values ($y^+ \approx 1$), very fine grid was taken near the top wall, bottom wall, and the injector plane. In the simulation, X-axis was taken in the longitudinal direction and Y-axis was taken along the vertical direction.

Supersonic conditions corresponding to Mach 2.44, static temperature of 1270 K, and static pressure of 1 atmosphere was imposed in the inflow plane. Sonic condition was imposed for hydrogen jet. Static temperature of the hydrogen jet was varied from 300 K to 800 K depending on the mixing and combustion cases. Static pressure of 1 atmosphere was fixed at the hydrogen inlet boundary. For mixing case, the composition of vitiated air stream contained N_2 and H_2O with mole fraction of 0.678 and 0.322, respectively. For combustion case, vitiated

air stream was composed of H_2O , O_2 and N_2 with mole fraction of 0.373, 0.199, and 0.428, respectively. Since, the outflow boundary is supersonic; the flow variables were obtained by extrapolation from the interior values. No information could be obtained for the inflow turbulence for the test conditions. The turbulence intensity and the ratio of turbulent to laminar viscosity were found from the sensitivity analysis and were set as (2.5 per cent, 350) and (2 per cent, 200) for the vitiated air stream and hydrogen stream respectively. Turbulent Schmidt number and Prandtl numbers are assumed as 0.7 and 1.0, respectively.

4.2 Simulation of the Mixing Case

Grid convergence of the solution was studied considering three different grids of sizes 300×130 , 260×110 , and 200×90 . The axial distribution of non-dimensionalised lower surface pressure is compared in Fig. 3, with three different grids. The surface pressure was non-dimensionalised by $P_{nozzle} = 0.917 \times 10^5$ Pa. But for the small region near the entry, the bottom wall surface pressure remains constant. It can be observed that by changing the grids to nearly 2 times, the results do not change much. The axial distribution of error estimate of the solution based on grid convergence index is also presented in the Fig. 3. For steady-state boundary-value problem, the main source of numerical error in CFD is iterative convergence or grid convergence error²⁷. Grid convergence or discretisation error, which is the error of the solution of the difference equations compared to the exact solution of the partial differential equation, is the major source of numerical error. This error can be estimated by running the solution in two different grids (coarse and fine). The simplest of such estimate is given by the relative difference $\epsilon = (f_2 - f_1)/f_1$, where f represent any quantity of interest and the indices 1 and 2 refer to the fine and coarse grid solutions, respectively.

Roache²⁸ has proposed a grid-convergence index (GCI) as an error based on uncertainty estimate of the numerical solution as

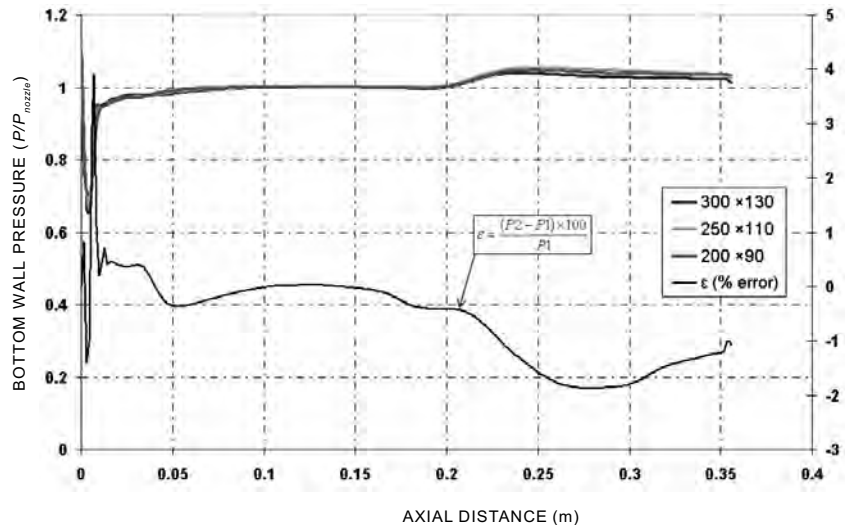


Figure 3. Axial distribution of surface pressure and error estimate for two grids ($P_{nozzle} = 0.917 \times 10^5$ pa).

$$GCI = F_s \frac{1\epsilon l}{(h_2/h_1)^p - 1} \quad (4)$$

where h is the order of grid spacing, p is the order of accuracy of numerical scheme and F_s is a factor of safety. Roache²⁹ has suggested $F_s = 3$ for minimal of two grid calculations. For the present calculation, $p = 2$ with $h_2/h_1 = 2.2$, GCI is order of 0.3ϵ . Maximum error between two simulations is within 4 per cent. This analysis indicates that the grid is adequate to capture most of the features of the flow and the solution in grid independent. Profiles of static temperature at the exit section of the combustor with three different grids are shown in Fig. 4. A very good match of the profiles with three different grids was observed.

The qualitative features of the flow field in the combustor are presented in the composite picture of static pressure and hydrogen mole fraction distribution in Fig. 5. From the static pressure contour it is observed that the expansion wave from the top of injector is hitting the upper wall at $X = 210$ mm. The wave from the upper wall is seen to interact with expansion wave at $X = 103$ mm and $Y = 57$ mm. Hydrogen stream is seen adhering to the lower wall. The diffusion of hydrogen is limited to $Y = 25$ mm at the exit of the combustor.

Various turbulence models namely Spalding's $k-\epsilon$ ³⁰, RNG $k-\epsilon$ ³¹, Realisable $k-\epsilon$ ³², Wilcox $k-\omega$ ³³, and Menter's $k-\omega$ ³⁴ were used to study the effect of various turbulence models in the flow. The exit profile of H_2 mole fraction with various turbulence models is compared in Fig. 6. Wilcox $k-\omega$ turbulence model outperforms other models as it predicts the mole fraction of species closer to the experimental value. It is expected as Wilcox $k-\omega$ turbulence model predicts the near-wall behaviour better than other models. All other models overpredict the species diffusion in the zone of 5 mm to 20 mm in the wall. Further calculations were carried out with Wilcox $k-\omega$ turbulence model. The computed pitot pressure at the exit of the combustor was compared with the experimental value in Fig. 7. A very good agreement between the two was observed.

The computed profiles of H_2 , N_2 and H_2O volume fractions at the combustor exit have been compared with the experimental values in Fig.8. A very good match between the experimental and computed values is observed. The lateral diffusion of all the species are well captured in the simulation although the computed H_2 volume fraction slightly underpredicts and N_2 and H_2O volume fraction slightly overpredicts the experimental values near the lower wall from

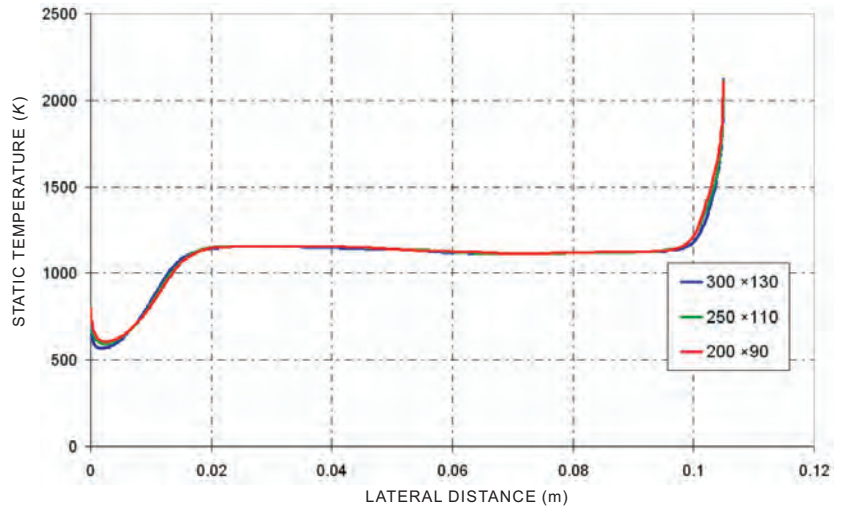


Figure 4. Static temperature profile at combustor exit with three different grids.

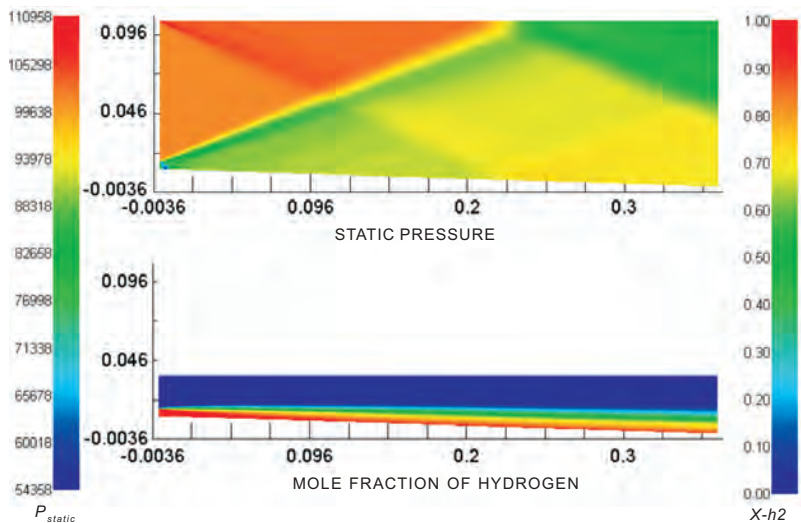


Figure 5. Distribution of static pressure and hydrogen mole fraction.

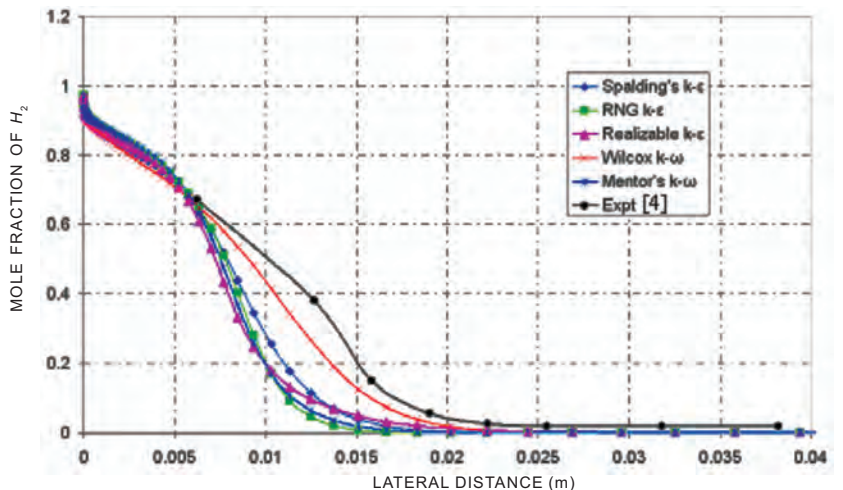


Figure 6. Comparison of exit profile of H_2 with various turbulence models.

12 mm to 18 mm lateral distance. To find out the sensitivity of turbulent Schmidt number on the species diffusion, simulations were carried out with different turbulent Schmidt numbers 0.25, 0.5, 0.7, and 1.0. The exit profile of hydrogen volume fraction with different Schmidt numbers is compared with experimental data in Fig. 9. It has been observed that the computed exit profile with $Sc_t = 0.5$ agrees better with the experimental data. Baurle and Eklund³⁵ also reported the strong dependence of Sc_t on prediction of supersonic mixing and combustion.

4.2 Simulation of Reacting Case

Two different chemical kinetics models namely, infinite fast rate kinetics and single-step finite rate chemistry were employed to find out the effect of chemical kinetics in the combustion characteristics in the flow field. The Mach number distribution in the combustor between the two cases has been compared in Fig. 10. Mach number distribution for the mixing case has also been plotted in the figure. Comparing the Mach number distribution between the three cases, it becomes clear that the reaction is confined near the lower wall. Most of the combustor width remains unaffected. For the finite rate chemistry, since the heat release is delayed, the reduction of Mach number is less near the inflow plane. Static temperature distribution in the combustor for the fast chemistry, finite rate chemistry, and no reaction case is presented in the Fig. 11. The reaction pattern is different between the fast chemistry and finite rate chemistry. Increase in temperature is seen at $x = 14$ mm for the fast chemistry, whereas for the finite rate chemistry, temperature is seen to increase for $x = 225$ mm. As expected, delayed reaction is observed for finite rate case compared to the fast reaction case. The backward reaction present in the single-step finite rate chemistry is endothermic in nature. The heat absorption by the backward reaction is causing the delay in ignition. In the fast chemistry calculation, the heat release is instantaneous; therefore, the ignition is occurring much earlier in the upstream region. The water mole fraction distributions for fast chemistry and finite rate chemistry are presented in Fig. 12. Significant water mass fraction is initiated at $x = 225$ mm for finite rate chemistry compared to $x = 14$ mm for fast rate chemistry. The temperature distribution and water mass fraction distribution correlate well. This is due to the assumption of normal diffusion (unity Lewis number) in the simulation. Ignition distance for the reacting case is measured in the experiment from the photographic measurement of OH radicals, which indicate that

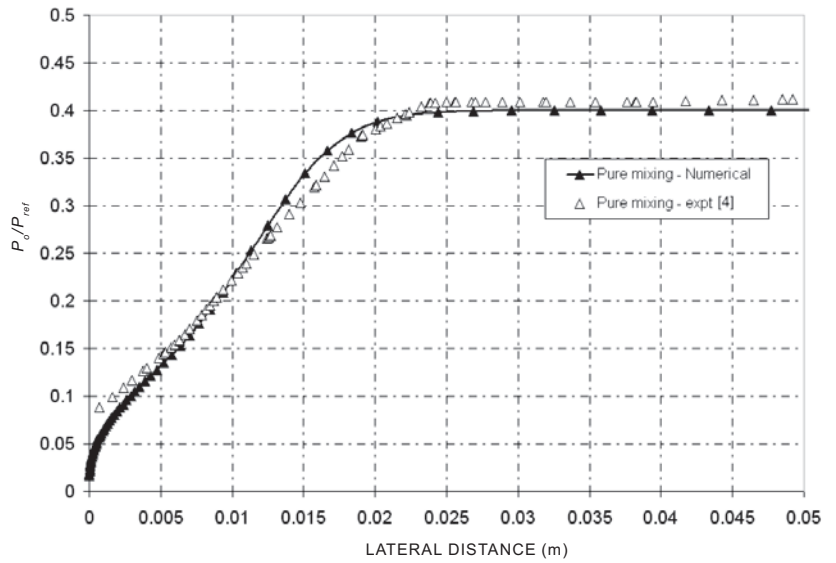


Figure 7. Pitot pressure profiles for pure-mixing study.

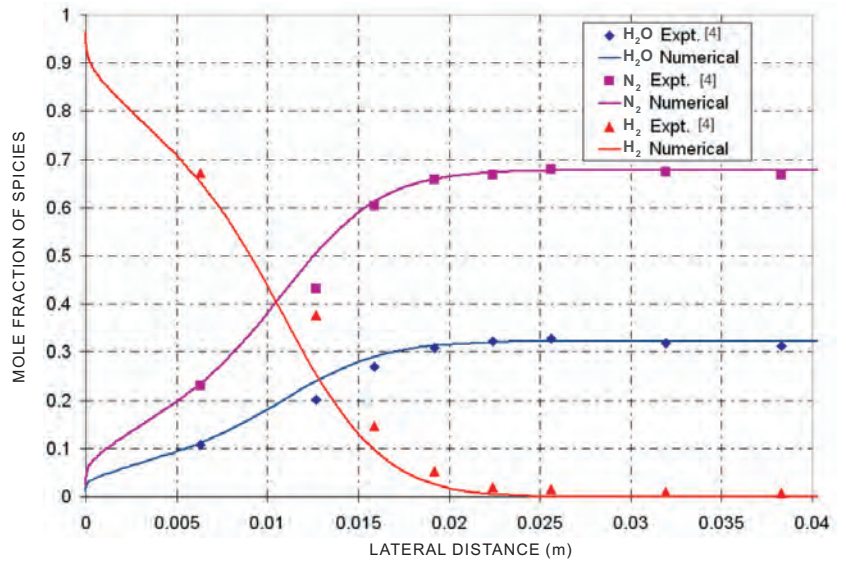


Figure 8. Comparison of computed and experimental volume fractions of H_2 , N_2 and H_2O at the combustor exit.

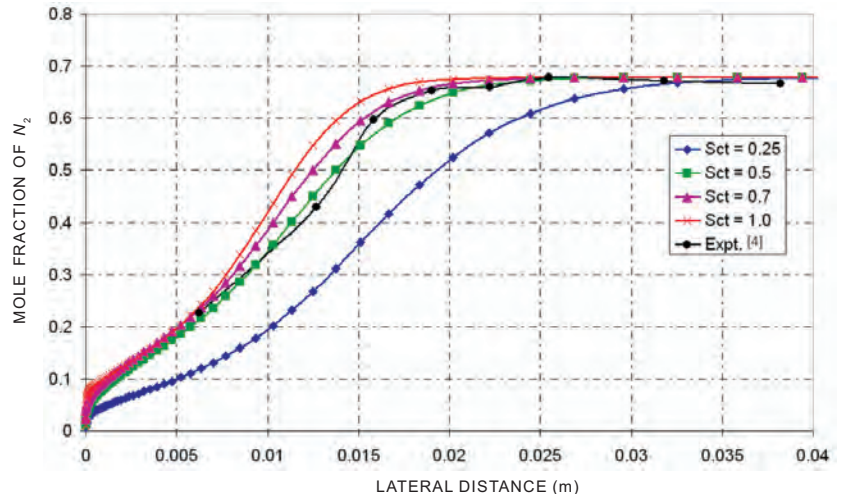


Figure 9. Comparison of exit profile of N_2 volume fraction with different Schmidt numbers Sc_t .

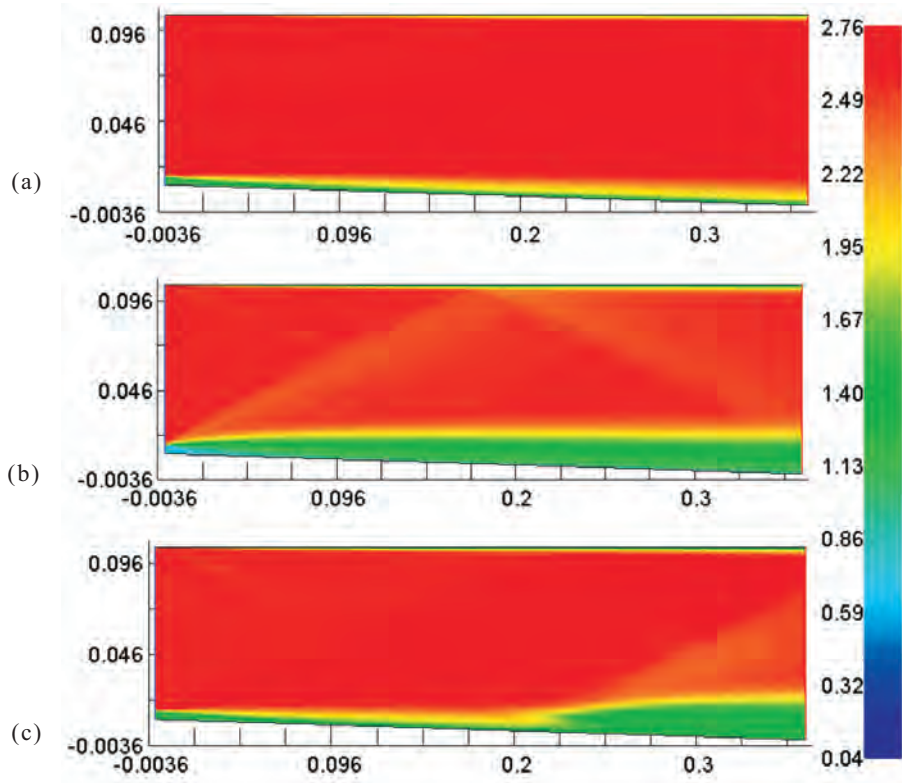


Figure 10. Mach number distribution in the combustor for the cases: (a) no reaction, (b) fast chemistry, and (c) finite rate chemistry.

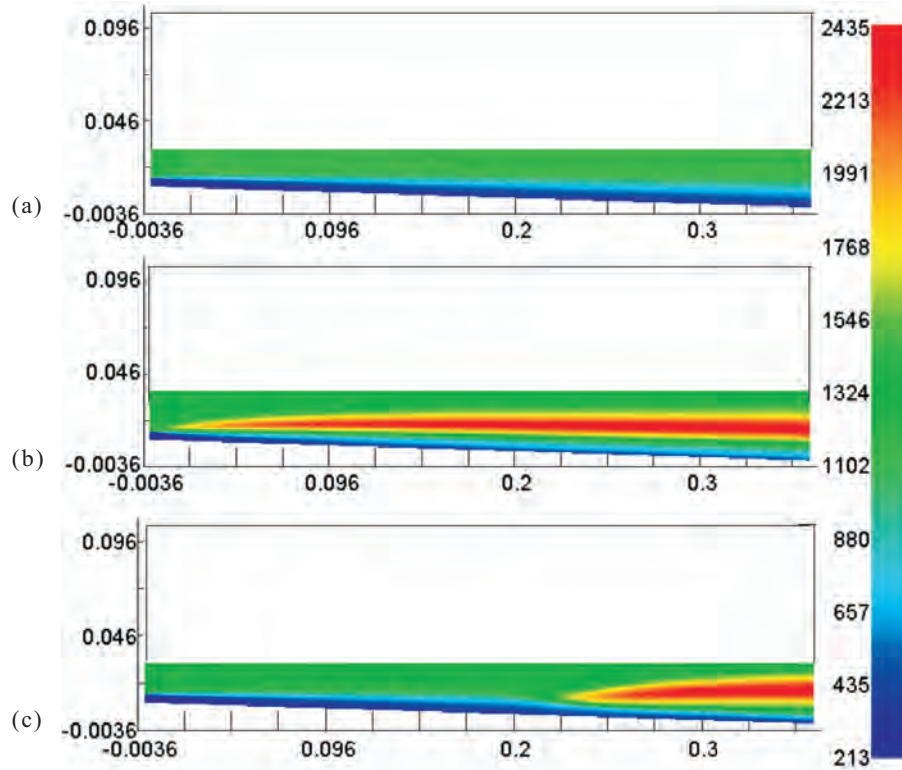


Figure 11. Static temperature distribution in the combustor for the cases: (a) no reaction, (b) fast chemistry, and (c) finite rate chemistry.

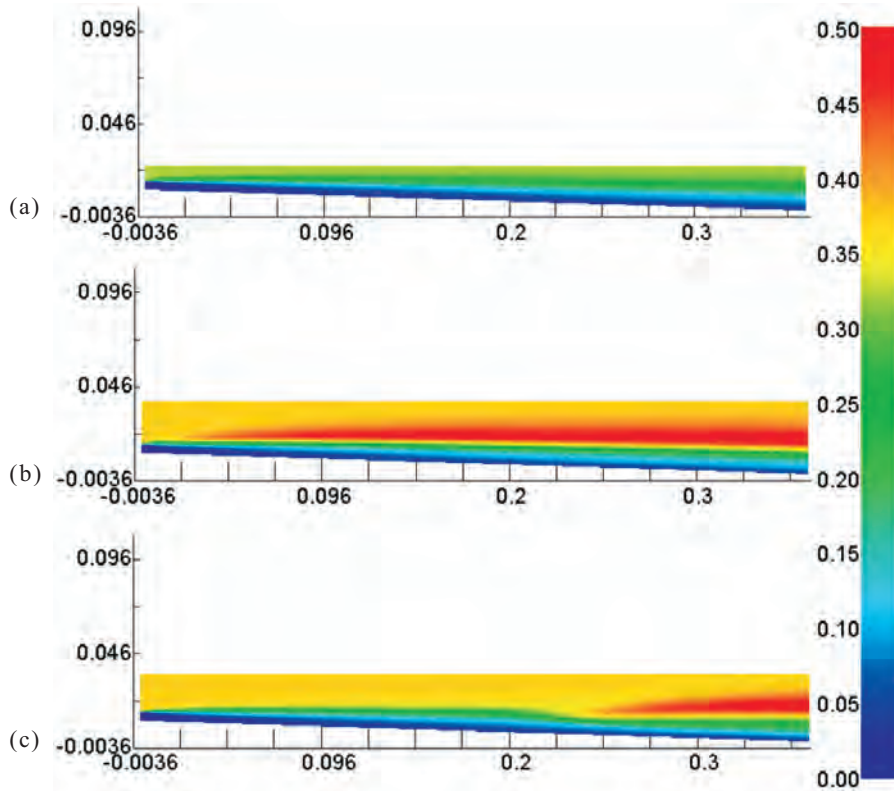


Figure 12. Mole fraction of H_2O : (a) non-reacting, (b) fast chemistry, and (c) finite rate chemistry.

ignition distance for the present case (local static temperature 1270 K) is about 250 mm from the inflow. Very good match is observed in ignition distance prediction between the computed (225 mm) and experimental (250 mm) data. This can be further improved with detailed multi-step finite rate calculations.

The axial distributions of combustion efficiency for different chemical schemes are presented in Fig.13. Following Kim,³⁶ *et al.* combustion efficiency is defined as

$$\eta_c(x) = 1 - \frac{\int \rho u Y_F dA}{(\rho u Y_F dA)_{x=0}} = 1 - \frac{m_F}{(m_F)_{x=0}} \quad (5)$$

where Y_F and m_F are the mass fraction and mass flow rate of hydrogen fuel, respectively.

The maximum combustion efficiency for $\phi=1.0$ is about 55 per cent. For lower equivalence ratios, the combustion efficiency is still higher.

The exit profile of H_2 and O_2 mole fraction obtained from the fast chemistry and finite rate chemistry has been compared with the experimental results in Fig. 14. Although overall trend is matching, both fast chemistry and finite rate chemistry underpredict the H_2 mole fraction compared to the experimental results. In the mid of the reaction zone ($y > 0.008$ m), predicted mole fraction with finite rate chemistry is slightly higher than the fast chemistry prediction. Near the wall ($y \approx 0.005$ m) as the temperature is low, reactions are slow for single-step finite rate chemistry; hence oxygen

is not getting consumed. This phenomenon is well captured by finite rate chemistry calculations. In infinite fast chemistry, oxygen is seen consumed instantaneously. Between $Y=0.015$ m to 0.25 m, the fast chemistry over predicts O_2 - mole fraction compared to the experimental results. The comparison of exit profile of H_2O and N_2 mole fraction between finite rate chemistry, fast chemistry, and the experimental values are given in Fig. 15. The computed water mole fraction peak is shifted towards the bottom wall. Single-step finite rate chemistry performs marginally better than fast rate kinetics. Water mass fraction exit profile with different

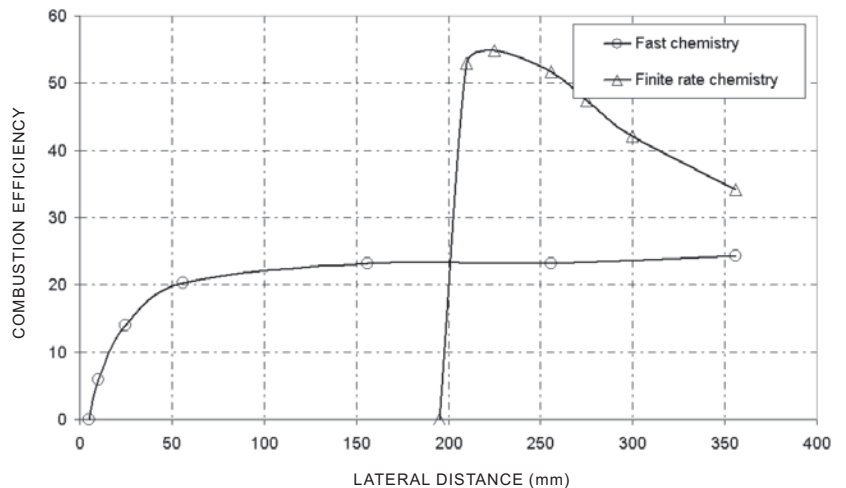


Figure 13. Axial distribution of combustion efficiency with different chemical schemes.

turbulent Schmidt numbers is presented in Fig. 16. It has been observed that the computed exit profile with $Sc_t = 0.5$ agrees better with the experimental data. Supersonic mixing and combustion is seen to depend strongly on Sc_t , which is consistent with the observation of other researchers³⁵.

5. CONCLUSIONS

Mixing and combustion of parallel hydrogen fuel into supersonic vitiated air stream in a divergent duct is simulated numerically. Three-dimensional Navier stokes equations are solved in multi-block structured grid using commercial CFD software. Different turbulence models are used to find their predictive capability of turbulent reacting flows. H_2 -air chemical reaction is modelled by employing two different chemical kinetics namely; infinitely fast rate kinetics and single-step finite rate chemistry and thermochemical behaviour of the flow field between the two have been compared. EDC-based finite rate combustion model was employed to describe turbulence chemistry interaction. Grid convergence of the solution has been established by carrying out the simulation with three different grids and comparing the results. An error estimate in terms of GCI shows that the maximum error between two simulations is within 2 per cent. Simulation captures all the essential features of the flow field. $K-\omega$ turbulence model performs the best amongst the turbulence models tested. Very good comparisons have been obtained for the exit profiles for various fluid dynamical and chemical variables for the mixing case. Single-step finite rate chemistry performs reasonably well in predicting the overall mixing and combustion process in the combustor. Computed temperature and species mole fraction distribution with single-step finite rate chemistry matches better with experimental results than the infinitely fast kinetics. Parametric studies with different turbulent Schmidt numbers show strong dependence of flow behaviour on modelled level of turbulent mass transfer. The results indicate that simple chemical kinetics is adequate to describe the H_2 -air reaction in the scramjet combustor.

REFERENCES

1. Ferri, E. Review of problems in application of supersonic combustion. *J. Royal Aero. Soc.*, 1964, **68**(645), 575-97.
2. Curran, E.T. Scramjet engines: The first forty years. *J. Propul. Power*, 2001, **17**(6), 1138-148.
3. Seiner, M; Dash, S.M. & Kenzakowski, D.C. Historical survey on enhanced mixing in Scramjet engines. *J. Propul. Power*, 2001, **17**(6), 1273-286.

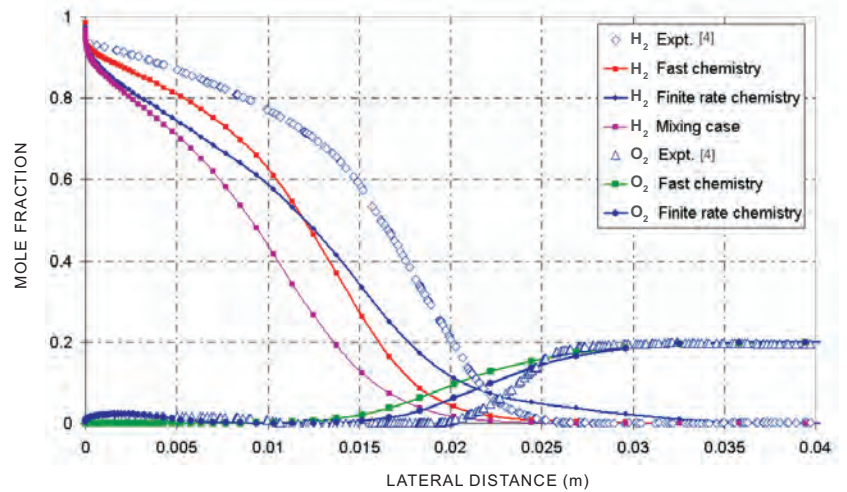


Figure 14. Comparison of exit profile of H_2 and O_2 mole fraction for: fast chemistry, finite rate chemistry, mixing case, and experiment.

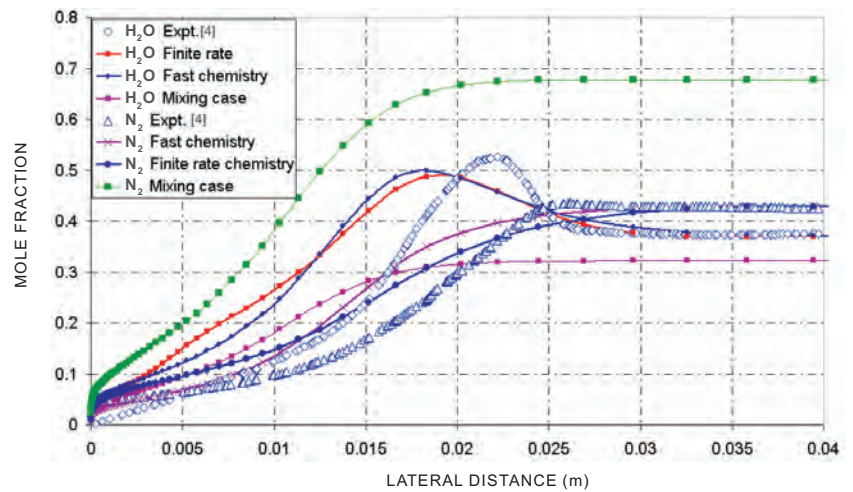


Figure 15. Comparison of exit profile of H_2O and N_2 mole fraction between: fast chemistry, finite rate chemistry, experiment.

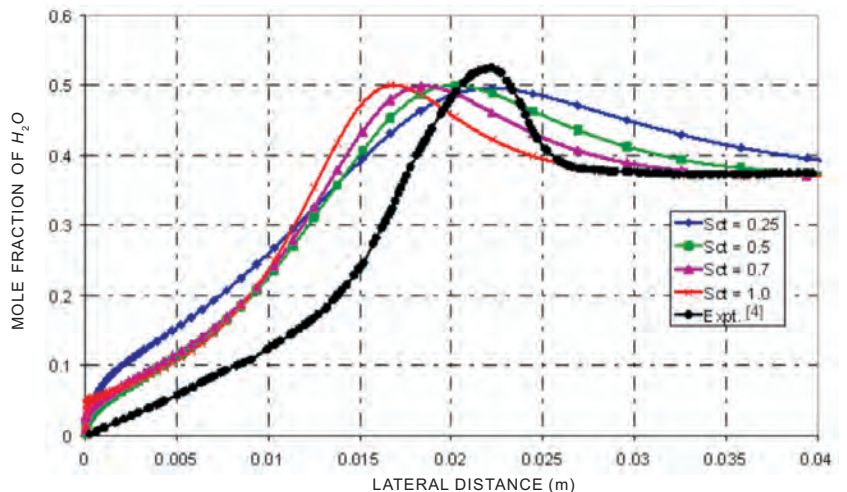


Figure 16. Variation of water mole fraction at combustor exit with turbulent Scimidth number.

4. Burrows, M.C. & Kurkov, A.P. Analytical and experimental study of supersonic combustion of hydrogen in vitiated air stream. Report No. NASA-TMX-2828, 1973.
5. Cheng, T.; Wehrmeyer, J.; Pitz, R.; Jarrett, O. & Northam, G. Finite rate chemistry effects in a Mach 2 reacting flow. AIAA Paper 91-2320, 1991.
6. Erdos, J.; Tamagno, J.; Bakos, R. & Trucco, R. Experiments on shear layer mixing at hypervelocity conditions. AIAA Paper 92-0628, 1992.
7. Tomioka, S.; Murakami, A.; Kudo, K. & Mitani, T. Combustion tests of a staged supersonic combustor with a strut. *J. Propul. Power*, 2001, **17**(2), 293-300.
8. Drummond, J.P. Supersonic reacting internal flow field, numerical approaches in combustion modelling. *In Progress in aeronautics and astronautics, edited by E.S. Organ & J.P. Borris, AIAA, 1991, 135*, pp. 365-420.
9. Carpenter, M.H. Three-dimensional computations of cross flow injection and combustion in a supersonic flow. AIAA Paper 89-1870, 1989.
10. K Uenishi, K.; Rogers, R.C. & Northam, G.B. Three dimensional computation of transverse hydrogen jet combustion in a supersonic air stream. AIAA Paper 87-0089, 1987.
11. Chitsomboon T. & Northam, G.B. Computational fluid dynamics prediction of the reacting flowfield inside a subscale scramjet combustor. *J. Propul. Power*, 1991, **7**(1), 44-48.
12. Saha, Soumyajit & Chakraborty, Debasis. Reacting flow computation of staged supersonic combustor with strut injection. AIAA Paper 2006-3895, 2006.
13. Kim, S.W. Numerical investigation of chemical reaction-Turbulence interaction in compressible shear layer. *Combustion Flame*, 1995, **101**, 197-208.
14. Kim, S.W. & Jenson, T.J. Fluid flow of a row of jets in crossflow-A numerical study. *AIAA Journal*, 1993, **31**(5), 806-11.
15. Keislter, P.G. A variable turbulent Pandtl and Shmidt number model study for scramjet applications. North Carolina State University, USA, 2009. PhD Thesis.
16. Xiao, X.; Edwards, J.R.; Hassan, H.A. & Gaffney, R.L. Role of turbulent Prandtl number on heat flux at hypersonic Mach numbers. AIAA Paper 2005-1098, 2005.
17. Xiao, X.; Hassan, H.A. & Baurle, R.A. Modelling scramjet flows with variable turbulent Prandtl and Schmidt numbers. AIAA Paper 2006-0128, 2006.
18. Alexopoulos, G.A. & Hassan, H.A. A $k-\zeta$ (Enstrophy) compressible turbulence model for mixing layers and wall bounded flows. AIAA Paper 1996-2039, 1996.
19. Jachimowski, C.J. An analytic study of the hydrogen-air reaction mechanism with application to scramjet combustion. NASA Technical Paper 2781, 1988.
20. Connaire, M.O.; Curran, H.J.; Simmie, J.M.; Pitz, W.J. & Westbrook, C.K. A comprehensive modelling study of hydrogen oxidation. *Int. J. Chem. Kinetics*, 2004, **36**(11), 603-22.
21. Fluent 6.3 User's guide. Fluent Inc., Lebanon, NH, US, 2006.
22. Roe, P.L. Characteristic based schemes for the Euler equations. *Annl. Rev. Fluid Mech.*, 1986, **18**, 337-65.
23. Gran, I.R. Mathematical modelling and numerical simulation of chemical kinetics in turbulent combustion. University of Trondheim, Norway, 1994. PhD Thesis.
24. Chakraborty, Debasis; Paul, P.J. & Mukunda, H.S. Evaluation of empirical combustion models for high speed H_2 -air confined mixing layer using DNS data. *Combustion Flame*, 2000, **121**(1-2), 195-209.
25. Chakraborty, Debasis; Upadhaya, H.V.Nagraja; Paul, P.J. & Mukunda, H.S. Thermo-chemical exploration of two-dimensional reacting supersonic mixing layer. *Physics of Fluids*, 1997, **9**(11), 3513-522.
26. Chemkin@ 4.1.1 Application programming interface guide. Reaction Design Inc., San Diego, CA, USA, 2004.
27. Guide for the verification and validation of computational fluid dynamic simulation G-077-1998. AIAA, Reston, VA, 1998.
28. Roache, P.J. Verification and validation in computational science and engineering. Hermora Publishers, New Mexico. 1998.
29. Roache, P. J. Error bar for CFD. AIAA Paper 2003-0408, 2003.
30. Launder, B.E. & Spalding, D.B. Lectures in mathematical models of turbulence. Academic Press, London, England, 1972.
31. Yakhot, V. & Orszag, S.A. Renormalisation group analysis of turbulence, Part-I : Basic theory. *J. Sci. Comput.*, 1986, **1**(1), 1-51.
32. Shih, T.H.; Liou, W.W.; Shabbir, A.; Yang, Z. & Zhu, J. A New $k-\epsilon$ Eddy-viscosity model for high Reynolds number turbulent flows-model development and validation. *Computers Fluids*, 1995, **24**(3), 227-38.
33. Wilcox, D.C. Turbulence modelling for CFD. DCW Industries, Inc., La Canada, California, 1998.
34. Menter, F.R. Two-equation Eddy-viscosity turbulence models for engineering applications. *AIAA Journal*, 1994, **32**(8), 1598-605.
35. Baurle, R.A. & Eklund, D.R. Analysis of dual-mode hydrocarbon scramjet operation at Mach 4 – 6.5. *J. Propul. Power*, 2002, **18**(5), 990-1002.
36. Kim, J.H.; Yoon, Y.; Jenng, I.S.; Hwanil, Hug & Choi, J.Y. Numerical study of mixing enhancement by shock where in model scramjet engine. *AIAA Journal*, 2003, **41**(6), 1074-080.

Contributors



Mr M.S.R. Chandra Murty obtained his BTech (Mech Engg) from Regional Engineering College (REC), Warangal. He is currently working as Scientist D, in Computational Combustion Dynamics Division, Defence Research and Development Laboratory (DRDL), Hyderabad. His areas of work include heat transfer and computational fluid dynamics related to aerospace propulsion.



Mr R.D. Mishal obtained his MTech (Mech Engg) from REC, Warangal. Presently he is working as Head, Dept of Mechanical Engg at Defence Institute of Advanced Technology (DIAT), Pune. His research areas are: Heat transfer and gas turbines.



Dr Debasis Chakraborty obtained his PhD in Aerospace Engg from Indian Institute of Science, Bengaluru. Presently, he is working as Technology Director, Computational Dynamics Directorate, DRDL, Hyderabad. His current interests are CFD, aerodynamics, high-speed combustion, and propulsion.